Supporting Information

Zirconium-amino acid framework as a green phosphatase-like nanozyme for selective detection of phosphate-containing drugs

Yuxin Wu,[‡a] Ting Huang,[‡a] Yuefei Luo,[a] Ling Dai,[b] Min Wang,*[a] Zhining Xia,[a] and Lianzhe Hu*[b]

[a] School of Pharmaceutical Sciences, Chongqing University, Chongqing, 401331,China.

[b] Chongqing Key Laboratory of Green Synthesis and Applications, College of Chemistry, Chongqing Normal University, Chongqing 401331, China.

* Corresponding author. E-mail: wang_min@cqu.edu.cn; lianzhehu@cqnu.edu.cn

[‡] These authors contributed equally to this work.

Experimental Section

Reagents and materials

Zirconium chloride ($ZrCl_4$) and risedronate sodium (RIS) were purchased from Aladdin Biological Technology Co., Ltd. (Shanghai, China). Zirconium hydroxide [$Zr(OH)_4$], 4-nitrophenyl phosphate (*p*-NPP) disodium salt hexahydrate and 4-methylumbelliferone (4-MU) were obtained from Yuanye Biotechnology Co., Ltd. (Shanghai, China). Alendronate sodium (ALDS) was purchased from Maclin Biochemical Technology Co., Ltd. (Shanghai, China). Combretastatin A4 disodium phosphate (CA4P) was purchased from Nantong Feiyu Biotechnology Co., Ltd. (Jiangsu, China). L-aspartic acid (L-Asp), ibuprofen, carbamazepine, memantine, metformin, cimetidine, dexamethasone, novobiocin, dipyrone, aciclovir, ranitidine, and nicotinic acid were purchased from Solarbio Technology Co., Ltd. (Beijing, China). Alkaline phosphatase (ALP) and 4-methylumbelliferyl phosphate (4-MUP) disodium salt were provided by Sigma-Aldrich Chemical (St. Louis, MO). 4-(2-hydroxyethyl)-1-piperazineethanesulfonic acid (HEPES) was purchased from Saiguo Biotechnology Co., Ltd. (Guangzhou, China). All aqueous solutions were prepared with deionized water (18.2 MΩ·cm, Millipore).

Apparatus

The fluorescence spectra were acquired on an F-7000 fluorescent spectrophotometer (Hitachi, Japan). The UV-visible absorption spectra were obtained with a UV2600 spectrophotometer (Shimadzu, Japan). Dynamic light scattering (DLS) and zeta potential measurements were carried on a Nanobrook Omni particle sizer and zeta potential analyzer (Brookhaven, USA). Scanning electron microscopy (SEM) images were collected on a Hitachi S-4800 field-emission scanning electron microscope (Hitachi, Japan). X-ray diffraction (XRD) measurement was obtained on a PANalytical X'Pert Powder diffractometer (PANalytical, Netherlands). X-ray photoelectron spectroscopy (XPS) measurements were taken on an ESCALAB 250Xi spectrometer (Thermo Fisher Scientific, UK). Determination of Zr element is performed on an inductively coupled plasma-optical emission spectrometer (ICP-OES)

(iCAP 6300 Duo, Thermo Fisher Scientific, UK).

Preparation of MIP-202(Zr)

MIP-202(Zr) was synthesized as previously described.[1] Briefly, 2.66 g L-Asp (20 mmol) and 5 mL water were added into a 25 mL round bottom flask. 2.33 g $ZrCl_4$ (10 mmol) was then added into the above L-Asp suspension. Another 5 mL water was introduced to bring the $ZrCl_4$ powder on the inner wall of the flask into the solution, followed by stirring until a clear colorless solution was obtained. Finally, the reaction was kept at reflux for 2 h at 120 °C under stirring. After cooling down to room temperature, the white solid MIP-202(Zr) was obtained by centrifugation, washed with 1:1 (v/v) water/ethanol for three times and dried in a vacuum oven.

Phosphatase-like catalytic activity of MIP-202(Zr)

By using *p*-NPP as the chromogenic substrate, kinetic measurements were performed with 80 μg/mL MIP-202(Zr) in 20 mM HEPES buffer solution (pH 8.5) containing100 μM *p*-NPP. The absorbance at 405 nm in time-scan mode was monitored for 20 min at room temperature. By using 4-MUP as the fluorogenic substrate, kinetic measurements were performed with 80 μg/mL MIP-202(Zr) in 20 mM HEPES buffer solution (pH 8.5) containing 5 μM 4-MUP. The fluorescence intensity at 448 nm in time-scan mode was monitored for 7 min at room temperature under excitation at 360 nm.

For the phosphatase-like activity comparison of MIP-202(Zr) with $ZrCl_4$ and $Zr(OH)_4$, kinetic measurements were performed with 80 μg/mL MIP-202(Zr), 50 μg/mL $ZrCl_4$ or 35 μg/mL $Zr(OH)_4$ in 20 mM HEPES buffer solution (pH 8.5) containing 5 μM 4-MUP. The fluorescence intensity at 448 nm in time-scan mode was monitored for 7 min at room temperature under excitation at 360 nm.

To explore the effect of solution pH on the catalytical activity of MIP-202(Zr) and ALP, MIP-202(Zr) and ALP were incubated at different pH values (i.e. pH 2.5, pH 4.0, pH 5.5, pH 7.0, pH 8.5 and pH 10) for 2 h, and then the activities were evaluated with 80 μg/mL MIP-202(Zr) or 10 ng/mL ALP in 20 mM HEPES buffer solution (pH 8.5) containing 5 μM 4-MUP. To study the thermal stability of MIP-202(Zr) and ALP, MIP-202(Zr) and ALP were first incubated in 20 mM HEPES buffer (pH 8.5) at

different temperatures (i.e. 25, 30, 40, 50, 60, 75 and 90 ^{o}C) for 2 h, and then their catalytic activities were tested at room temperature. For the Michaelis-Menten curves, the initial velocity of the reaction was calculated according to the kinetic measurements and the standard curve of 4-MU. The Michaelis-Menten constant K_m and V_{max} was deduced from the Lineweaver-Burk plots.

Fluorescence detection of phosphate-containing drugs

As a proof-of-concept, ALDS is chosen as the model phosphate-containing drug and ALDS measurements were performed with 80 μg/mL MIP-202(Zr) in 20 mM HEPES buffer solution (pH 8.5) containing 5 μM 4-MUP and different concentrations of ALDS in a range of 0-20 μg/mL (i.e. 0, 0.01, 0.03, 0.05, 0.08, 0.1, 0.3, 0.5, 1, 2 , 3 , 4, 5, 8, 10 and 20 μg/mL). The fluorescence intensity at 448 nm in time-scan mode was monitored for 7 min at room temperature under excitation at 360 nm. To verify the generality of the strategy, the same steps as above were carried out for the detection of the other two phosphate-containing drugs including RIS and CA4P, both of which contain the phosphate groups. The concentrations of RIS were 0, 0.5, 1, 2, 3, 5, 8, 10, 20, 40, 80, 120 and 200 μg/mL. The concentrations of CA4P were 0, 5, 10, 20, 40, 60, 80, 120, 160, 200 and 300 μg/mL. To verify the specificity of the strategy, 11 common drugs including ibuprofen, carbamazepine, memantine, metformin, cimetidine, dexamethasone, novobiocin, dipyrone, aciclovir, ranitidine, nicotinic acid were selected as interfering substances. Then the measurements were performed with 80 μg/mL MIP-202(Zr) in 20 mM HEPES buffer solution (pH 8.5) containing 5 μM 4-MUP and 10 μg/mL drug. The fluorescence intensities at 7 min were recorded. For simulating ALDS detection in real samples, the detection of ALDS in urine was also carried out. Briefly, the urine was diluted 50 times with 20 mM HEPES buffer solution (pH 8.5). Then different concentrations of ALDS (i.e. 0.01, 0.1 and 1 μg/mL) were spiked into the diluted urine, followed by testing according to the above ALDS measurements. Each error bar shows the standard deviation of three independent measurements.

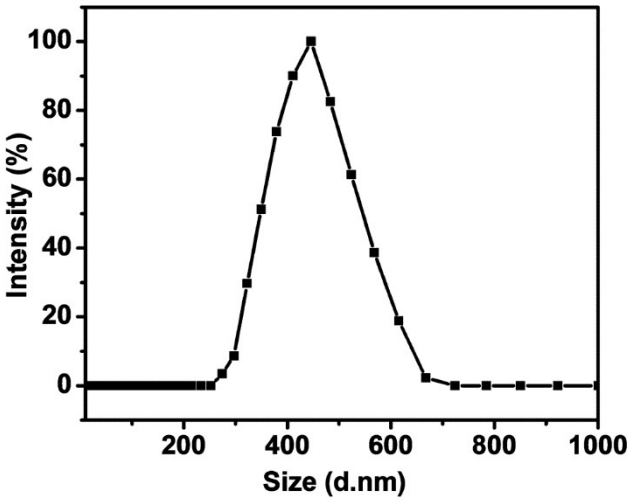

Fig. S1 The hydrodynamic size distribution of of MIP-202(Zr).

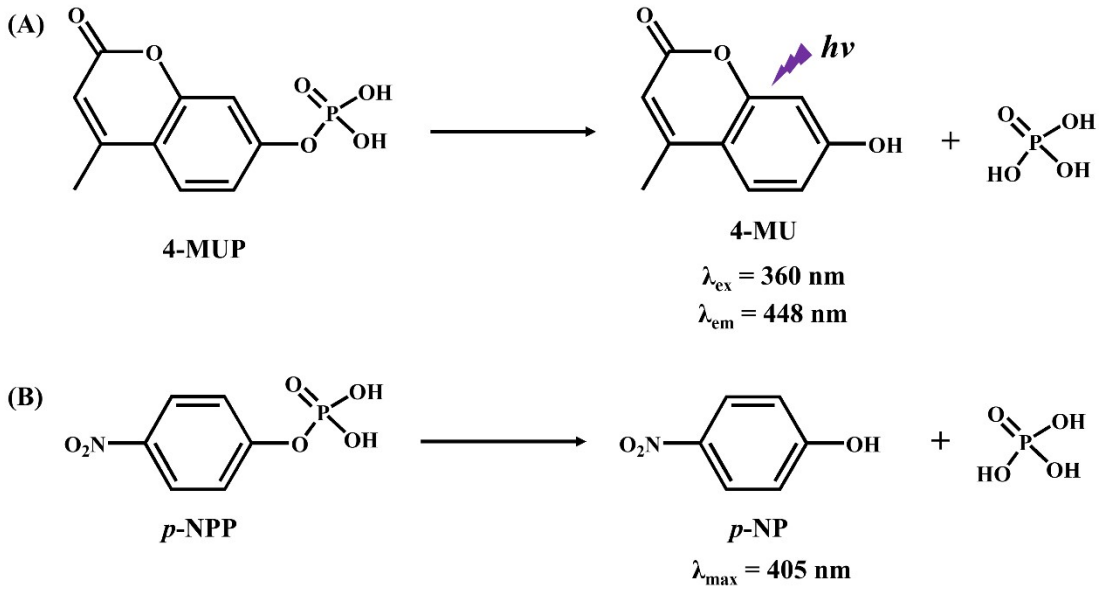

Fig. S2 Schematic of the dephosphorylation reaction of different substrates catalyzed by phosphatase or phosphatase mimics. (A) Dephosphorylation of the fluorescent substrate 4-MUP; (B) Dephosphorylation of the chromogenic substrate *p*-NPP.

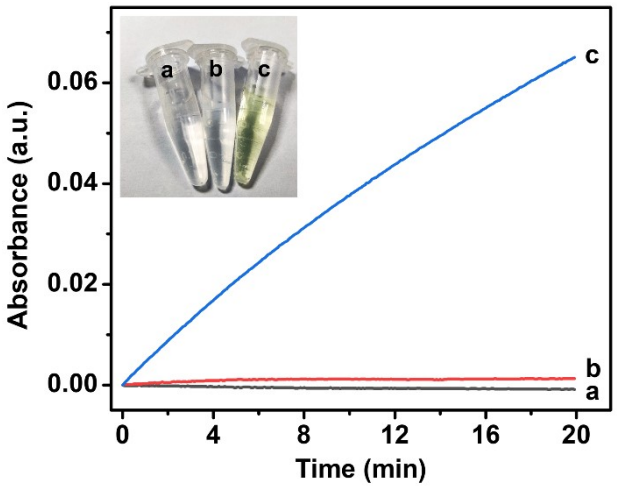

Fig. S3 (A)Time-dependent absorbance change of 20 mM HEPES buffer (pH 8.5) (a), 100 μM *p*-NPP (b) and 100 μM *p*-NPP in the presence of 80 μg/mL MIP-202(Zr) (c) at 405 nm. Inset: the corresponding photo of the three solutions.

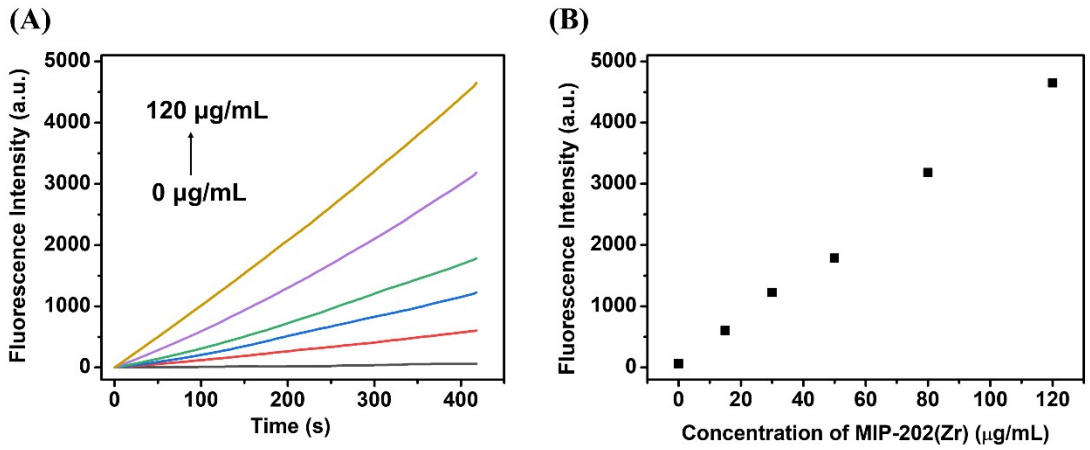

Fig. S4 (A) Time-dependent fluorescence change of 5 μM 4-MUP in the presence of different concentrations of MIP-202(Zr) (i.e. 0, 15, 30, 50, 80 and 120 μg/mL). (B) The plot of fluorescence intensity at 7 min versus MIP-202(Zr) concentration.

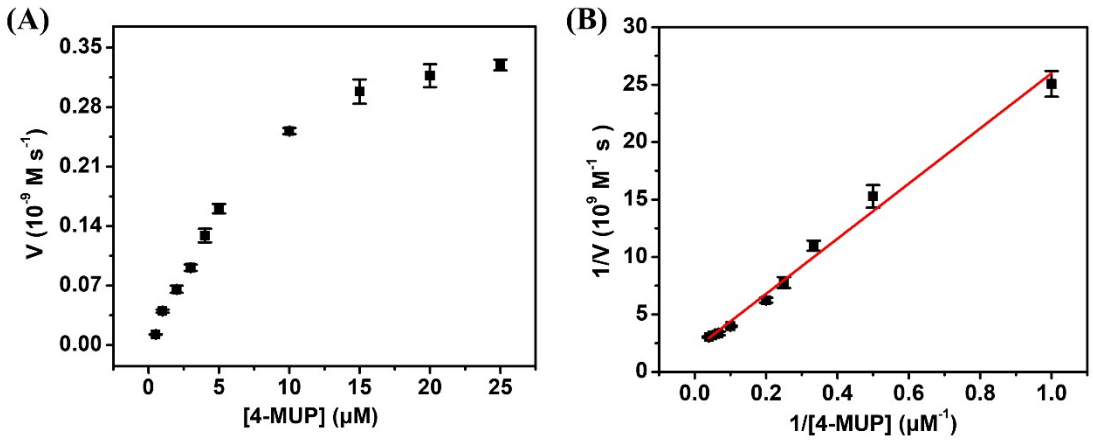

Fig. S5 (A) Steady-state kinetic assay of MIP-202(Zr) by varying concentration of 4-MUP (i.e. 0.5, 1, 2, 3, 4, 5, 10, 15, 20 and 25 μM). (B) Lineweaver-Burk plot of MIP-202(Zr) obtained from Fig. S5A according to the double reciprocal of the Michaelis-Menten equations.

Table S1 Comparison of kinetic parameter K_m among MIP-202(Zr) with those of ALP and the reported phosphatase-like nanozymes.

Catalyst	K_m (μM)	Reference
ALP	2.31	This work
CeO_2 NPs	16.5	2
ZrO_2 NPs	14.7	2
MIP-202(Zr)	10.27	This work

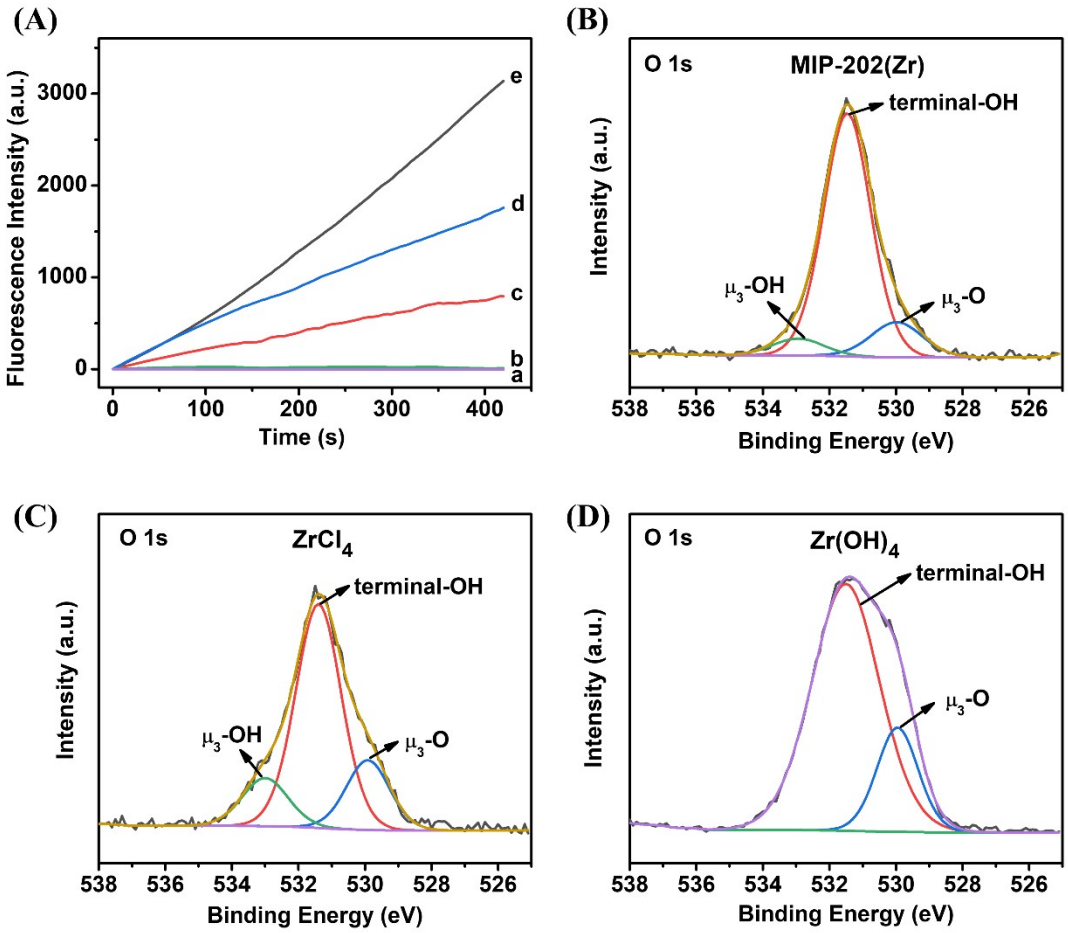

Fig. S6 (A) Time-dependent fluorescence change of 20 mM HEPES buffer (pH 8.5) (a), 5 μM 4-MUP in the presence of the supernatant of 80 μg/mL MIP-202(Zr) (b), 35 μg/mL $Zr(OH)_4$ (c), 50 μg/mL $ZrCl_4$ (d) and 80 μg/mL MIP-202(Zr) (e). The high-resolution XPS spectra of the O1s region of MIP-202(Zr) (B), $ZrCl_4$ (C) and $Zr(OH)_4$ (D).

Table S2. Binding energies and relative contents of fitting peaks in O 1s region of MIP-202(Zr), $ZrCl_4$ and $Zr(OH)_4$.

	MIP-202(Zr)	$ZrCl_4$	$Zr(OH)_4$
μ_3-OH	532.94 eV	533.00 eV	-
	(6.16%)	(14.28%)	
terminal-OH	531.46 eV	531.40 eV	531.51 eV
	(80.96%)	(66.20%)	(79.53%)
μ_3-O	529.98 eV	529.92 eV	529.96 eV
	(12.88%)	(19.52%)	(20.47%)

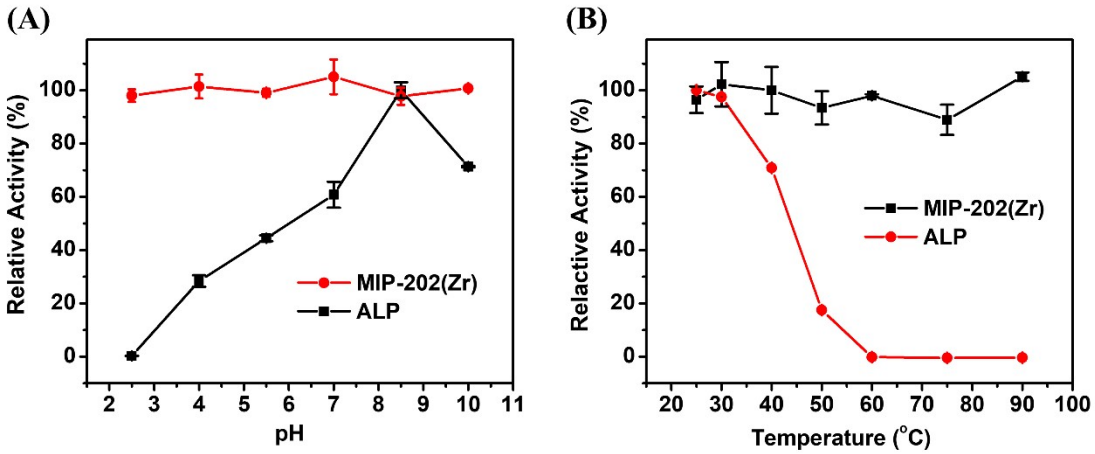

Fig. S7 The effect of pH (A) and temperature (B) on the stability of catalytic activities of MIP-202(Zr) and ALP. MIP-202(Zr) and ALP were incubated at pH 2.5-10 or at 15-90 °C for 2 h, followed by the activity tests under standard conditions (25 °C, pH 8.5).

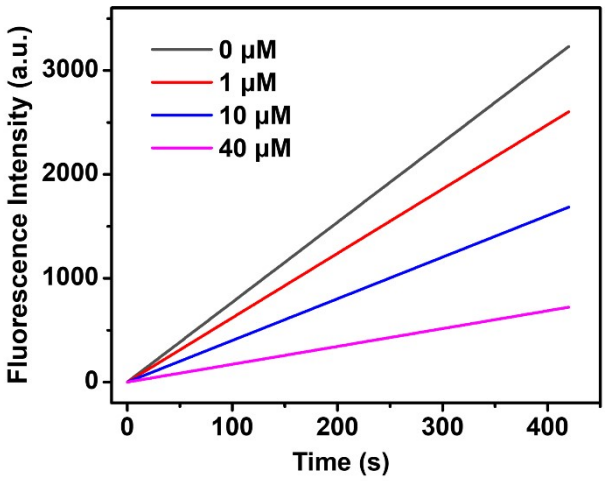

Fig. **S8** Time-dependent fluorescence change of MIP-202(Zr)/4-MUP system in the presence of different concentrations of phosphate (i.e. 0, 1, 10 and 40 μM).

Table S3. Comparison of the proposed method with other methods for ALDS detection.

Method	Probe	Linear range (ng/mL)	LOD (ng/mL)	Reference
Fluorescence	O-phthalaldehyde	130-780	2.89	3
Fluorescence	Terbium	40-800	33	4
Fluorescence	Iron (III)-alicylate	6500-29250	2437.5	5
Ratiometric fluorescence	GQDs-Ce^{4+}-OPD	3.25-325.12 325.12-32512	1.08	6
Ratiometric fluorescence	Ce^{4+}-AA-OPD	32.5-325.12 325.12-2275.8	9.75	7
Fluorescence	MIP-202(Zr)	10-100 100-3000	2	This work

Table S4. Results of determination of ALDS in urine by standard addition method.

Uric Samples	Spiked (μg/mL)	Found (μg/mL)	Recovery (%)	RSD (%)
1	0.01	0.0098	98.00	3.83
2	0.10	0.10	100.00	0.70
3	1.00	1.03	103.00	5.24

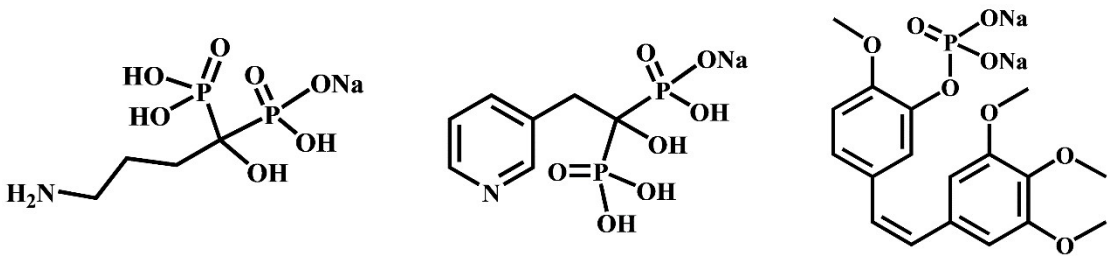

ALDS **RIS** **CA4P**

Fig. S9 Structural formulas of three phosphate-containing drugs ALDS, RIS and CA4P.

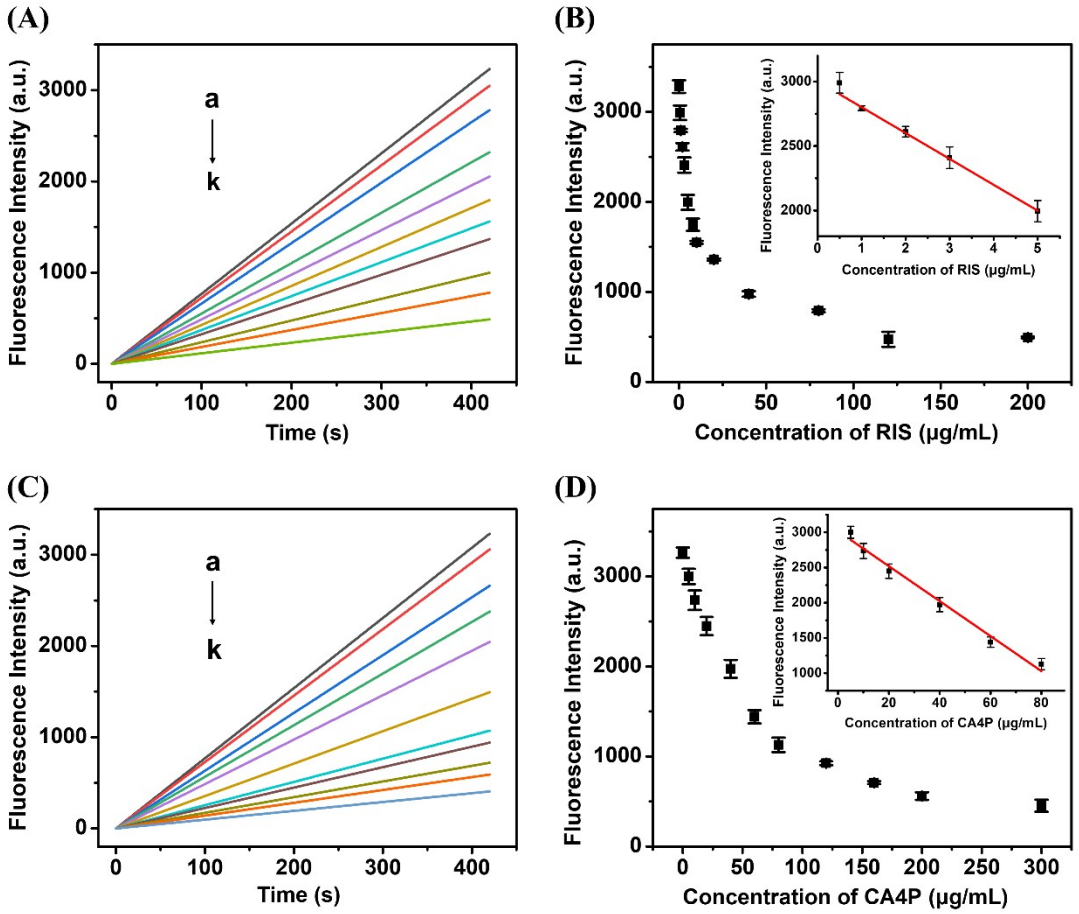

Fig. S10 (A) Time-dependent fluorescence change of MIP-202(Zr)/4-MUP system in the presence of different concentrations of RIS, from a to k: 0, 0.5, 1, 3, 5, 8, 10, 20, 40, 80 and 200 μg/mL. (B) The plot of fluorescence intensity at 7 min versus RIS concentration. The inset shows the linear relationship between the fluorescence intensity at 7 min and the RIS concentration in a range from 0.5 to 5 μg/mL. (C) Time-dependent fluorescence change of MIP-202(Zr)/4-MUP system in the presence of different concentrations of CA4P, from a to k: 0, 5, 10, 20, 40, 60, 80, 120, 160, 200 and 300 μg/mL. (D) The plot of fluorescence intensity at 7 min versus CA4P concentration. The inset shows the linear relationship between the fluorescence intensity at 7 min and the CA4P concentration in a range from 5 to 80 μg/mL.

References

1. S. Wang, M. Wahiduzzaman, L. Davis, A. Tissot, W. Shepard, J. Marrot, C. Martineau-Corcos, D. Hamdane, G. Maurin, S. Devautour-Vinot and C. Serre, *Nat. Commun.*, 2018, **9**, 4937.
2. X. L. Hu, T. Huang, H. Liao, L. Z. Hu and M. Wang, *J. Mater. Chem. B*, 2020, **8**, 4428-4433.
3. J. Ezzati Nazhad Dolatabadi, H. Hamishehkar, M. de la Guardia and H. Valizadeh, *BioImpacts*, 2014, **4**, 39-42.
4. N. Niaei, A. Samadi, H. Hamishehkar and M. Ghorbani, *Microchem. J.*, 2019, **146**, 888-894.
5. S. F. Elmalla and F. R. Mansour, *Luminescence*, 2019, **34**, 375-381.
6. M. Xia, X. E. Zhao, J. Sun, Z. J. Zheng and S. Y. Zhu, *Sensor. Actuat. B-Chem.*, 2020, **319**, 128321.
7. M. Xia, F. J. Shi, Y. H. Xia, J. Sun, X. E. Zhao and S. Y. Zhu, *Spectrochim. Acta A*, 2021, **251**, 119437.